SPINE Volume 31, Number 1, pp 44–50


# CT Imaging Techniques for Describing Motions of the Cervicothoracic Junction and Cervical Spine During Flexion, Extension, and Cervical Traction

Scott Simon, MD,* Martin Davis, MS,* Dewey Odhner, MA,† Jayaram Udupa, PhD,† and Beth Winkelstein, PhD*‡

**Study Design.** Computerized tomographic study of human cadavers undergoing traction and flexion-extension bending.

**Objectives.** To investigate the feasibility of using computerized tomography techniques to quantify relative vertebral motions of the cervical spine and cervicothoracic junction (CTJ), and to define normative CTJ kinematics.

**Summary of Background Data.** Despite developing an understanding of the mechanical behavior of the cervical spine, little remains known about the cervicothoracic junction. The CTJ is more difficult to image than other cervical regions given the anatomic features of the surrounding bones obstructing CTJ visualization. As such, limited data have been reported describing the responses of the CTJ for motions and loading in the sagittal plane, confounding the clinical assessment of its injuries and surgical treatments used at this region.

**Methods.** Helical CT images of the cervical spine and CTJ were acquired incrementally during each of flexion, extension, and cervical traction. Vertebral surfaces were reconstructed using the specialized image analysis software, 3DVIEWNIX. A mathematical description of relative vertebral motions was derived by computing rigid transformations. Euler angles and translations were calculated. Regional spine stiffness was defined for traction.

**Results.** The CTJ was found to be much stiffer (779 N/mm) than the cervical spine (317 N/mm) in tension. In flexion-extension bending, the CTJ was similar to the lower cervical spine. The CTJ demonstrated significantly less coupled motion than the cervical spine.

**Conclusions.** The CTJ, as a transition region between the cervical and thoracic spines, has unique kinematic characteristics. This application of kinematic CT methods is useful for quantifying unreported normative ranges of motion for the CTJ, difficult by other conventional radiologic means.

**Key words:** cervical spine, cervicothoracic junction, kinematics, imaging, computerized tomography, biomechanics. **Spine 2006;31:44–50**

The cervicothoracic junction (CTJ) is a unique spinal region, as it provides the transition between the highly flexible cervical spine and the more rigid thoracic region inferior to it. The CTJ is generally defined as the region of the collective joints of the lower cervical spine and the uppermost thoracic vertebra, C7–T1 or C7–T2.[1–4] Currently, there is a paucity of information describing CTJ mechanical behavior for both normal and injured conditions, limiting the understanding of CTJ injury mechanisms and evaluation of effective surgical treatments. While it is likely that the CTJ displays certain mechanical similarities with its adjacent counterparts, no study has reported CTJ mechanics for clinically relevant head kinematics and kinetics.

One of the challenges in studying the CTJ comes from distinct anatomic constraints to its direct visualization. While the lower cervical spine and CTJ are disproportionately affected by soft tissue injuries,[4–8] visualization of the individual vertebrae of the lower cervical spine and CTJ is quite difficult given obstruction by the scapulas and clavicle in lateral radiographic views.[9–12] Studies have used a variety of techniques, including planar radiographs,[9,13,14] goniometers in volunteer studies,[1] and direct measurements of dissected cadaveric specimens[15,16] to investigate spine kinematics. While these studies collectively provide useful information regarding spine kinematics, they provide only global relationships between head and torso movements, characterize only primary motions and do not examine coupled rotations or translations, or do not incorporate the CTJ region. Reports in the literature have compared the stiffness and effectiveness of various surgical instrumentation devices and fixation techniques across the CTJ.[10,17,18] However, these studies, while providing useful comparisons for surgical treatment options, do not report normative data for the CTJ region. Moreover, cadaveric studies are often isolated *ex vivo* and with the absence of paraspinal musculature or rib cage,[10,16,17,19,20] further limiting their interpretation or direct relevance to the clinical scenario. Recently, the use of three-dimensional magnetic resonance imaging (MRI) techniques has made possible the investigation of the kinematics of the upper and subaxial cervical spine in volunteers undergoing axial rotation,[21,22] pointing toward the utility of such advanced analysis of imaging methods for describing coupled motions in spinal regions, which are otherwise difficult to assess. However, despite the host of

From the *Department of Neurosurgery, †Medical Image Processing Group, Department of Radiology, and ‡Department of Bioengineering, University of Pennsylvania, Philadelphia, PA.
Acknowledgment date: September 20, 2004. First revision date: December 17, 2004. Acceptance date: January 19, 2005.
Supported by Synthes, Inc. and the Catharine D. Sharpe Foundation.
The manuscript submitted does not contain information about medical device(s)/drug(s).
Foundation funds were received in support of this work. No benefits in any form have been or will be received from a commercial party related directly or indirectly to the subject of this manuscript.
Address correspondence and reprint requests to Beth A. Winkelstein, PhD, 120 Hayden Hall, 3320 Smith Walk, Philadelphia, PA 19104. E-mail: winkelst@seas.upenn.edu

**Table 1. Specimen Anthropometric Data**

| Cadaver ID | Age (yr) | Height (cm) | Weight (kg) | Cause of Death |
|---|---|---|---|---|
| 592 | 71 | 178 | 111 | Cardiac arrest |
| 615 | 61 | 178 | 82 | Myocardial infarction |
| 576 | 51 | 188 | 82 | Intracranial bleed |
| 894 | 60 | 178 | 91 | Stroke |
| 903 | 69 | 175 | 68 | Cardiopulmonary arrest |
| 957 | 46 | 180 | 73 | Lung cancer |
| 945 | 69 | 178 | 82 | Colon cancer |

approaches for examining coupled spine motions, the normal kinematics of the CTJ have not been previously characterized.

Therefore, the purpose of this study was to implement stressed computerized tomography (sCT) techniques to quantify the three-dimensional motions of the cervicothoracic junction *in situ* for clinically relevant scenarios. Similar methods have been developed[23] and implemented[24] previously for MRI to describe kinematics for multiaxial joints, such as the ankle,[19] and have been shown to have utility in detecting variations in foot architecture, ligamentous injuries, and joint instability.[24,25] Such techniques offer particular utility for investigating the CTJ, especially since this region remains difficult to image using conventional techniques. This study quantifies CTJ motion in response to applied traction and flexion-extension, providing normative primary and coupled response data for this currently unstudied spinal joint complex. These loading paradigms were selected for initial investigation because coupled motions are limited to the sagittal plane.

## ■ Materials and Methods

Seven male unembalmed cadaveric head-neck-torso specimens, with arms and legs removed, were stored at −20° C until the time of testing. All cadavers were without any history of spinal pathology. The mean age at the time of death was 61 ± 10 years, and the mean weight was 84 ± 14 kg (Table 1). All specimens underwent incremental traction loading followed by incremental head flexion-extension.

For testing, the torso was rigidly fixed to the CT scanner table in a supine position. The head and neck were placed in a custom head frame in a neutral position, defined with the Frankfurt plane angled 15° from the vertical. Before any mechanical testing, the cervical spine was manually preconditioned with 30 cycles of flexion-extension bending applied at the head. Traction was applied with Gardner-Wells tongs, affixed to the skull according to clinical practice, with pins placed 2 cm above the pinna of the ear and in line with the tragus (Figure 1A). Weights were applied using a rope-and-pulley system fixed to a point outside the scanner gantry. Axial traction was applied in increments of 44.5 N up to 178 N. At each load increment, a creep time of 3 minutes was allowed before scan acquisition. For characterization of sagittal bending responses, a customized bending frame manipulated the head using pins placed in the ears to impose known flexion and extension rotations (Figure 1B). For this application, the torso was rigidly fixed to the torso portion of the base of the frame, and pins were tightly screwed into the auditory meatus to allow free head rotation and a controlled bending angle of the head relative to the torso. For these tests, the cervical spine was returned to neutral and the head underwent rotation at each of 0° (neutral), 10°, 20°, 30°, and 45° in flexion and 10°, 20°, and 30° in extension. At the completion of the test battery, the head was returned to neutral and data were reacquired for monitoring any rigid body motions that may have occurred during testing.

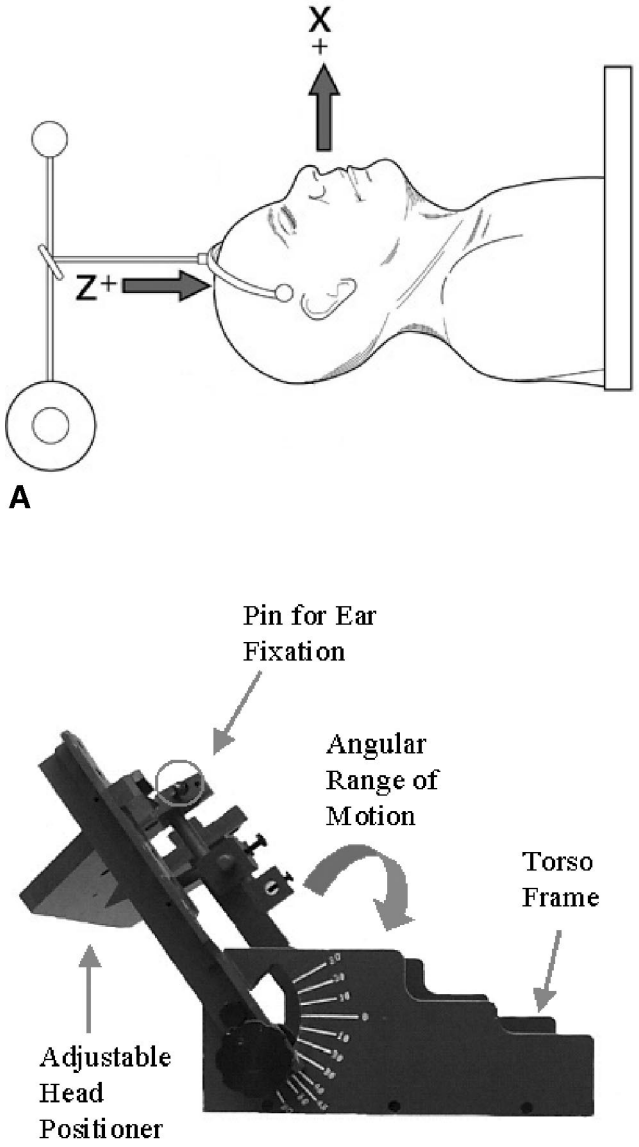


Figure 1. Illustration of testing devices and methods for applying head traction (**A**) and rotation (**B**) to specimens. A, For traction, Gardner-Wells tongs were applied to the head, and a series of weights were suspended from a pulley. B, A customized head frame was used to apply head rotation, with the torso fixed to the base of the frame and the head fixed to an adjustable positioner by means of pins placed in the ears, which allowed rotation only in the sagittal plane. Here the frame is shown in position for head flexion. Also shown in A, the global coordinate axis system: the positive x-axis is directed anteriorly, the positive y-axis is directed toward the specimen's right (out of the page), and the positive z-axis is directed inferiorly.

CT images were acquired in a Siemens Volume Zooming Multislice CT scanner (Siemens Medical Solutions, Malvern, PA). For all tests, scan images were obtained from the base of the occiput to the superior endplate of T3, at each increment of applied load or rotation detailed above. Each scanning series was obtained by using a 1.0-mm slice thickness, a slice spacing of 1.5 mm, and a pixel size of 0.23 to 0.35 mm. Scan time for each series was approximately 3 minutes. The scanner coordinate system served as the fixed coordinate system for motion analysis. In this system, the z-axis was defined along the superior-inferior direction, the y-axis in the medial-lateral direction, and the x-axis in the posterior-anterior direction (Figure 2).

The sCT technique in this study used the 3DVIEWNIX software system developed by one of the coauthors (J.U.).[26] This system facilitates the visualization, manipulation, and analysis of multidimensional image information. It was specifically adapted for the CTJ kinematic application with some modifications. This sCT technique consists of the following four key steps:

S1. Segmentation and separation of individual vertebra in the image: This is the only step that currently requires help from a knowledgeable human operator. The separation of the vertebral bodies, especially at the facets, is difficult by automatic means because the bony margins of the facets are in very close proximity to each other. This causes image blur and requires a human operator to indicate the separation. In our study, an operator drew a region of interest (ROI) on each slice in such a manner that only a given vertebra was within the ROI. The vertebra is segmented by intensity thresholding within the ROI.

S2. Construction of vertebral surfaces and principal axes: The binary image resulting from (S1) is subjected to a series of operations (including interpolation, filtering, and surface tracking) to construct the surface of each vertebral body. From this surface, the principal axes of the vertebra are determined according to the inertial axes of the bone based on the shape of the surface by considering all points on the surface, with the first principal axis oriented in the direction of greatest bone length/mass (in this case, approximately along the x-axis; Figure 2). The geometric centroid (as the origin), together with the principal axes, determines a local vertebral coordinate system.

S3. Motion analysis: A mathematical description of the relative motions of the individual vertebra is derived by computing the rigid transformation required to match the centroids and principal axes of the vertebral surfaces, in effect matching the two surfaces. This mathematical description allows for the measurement of individual vertebral and coupled three-dimensional movements; these measurements are reported as translations and Euler angles.

S4. Visualization: Surface renderings depicting the vertebrae in any configuration are then created along with the principal axes to allow visualization. For this study, visualization of motion is not provided; simply, relative vertebral kinematics are estimated.

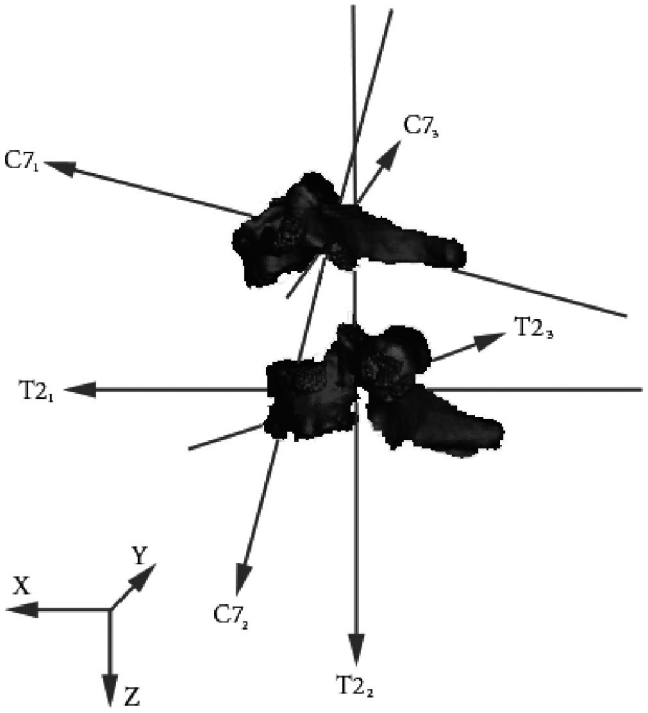


Figure 2. A reconstruction of the C7 and T2 vertebrae in the neutral position, with no rotation or traction, illustrating the principal axes (1, 2, 3) superimposed on the reconstructed spine segment. The principal axes have their origin at the centroid of each vertebra (C7, T2). The relative change in the location of the centroid and the orientation of the principal axes in the global frame (shown in the lower left hand corner) were used to determine the kinematics of the vertebrae.

This methodology in conjunction with MRI was previously used for studying the morphology, architecture, and kinematics of the ankle complex of normal feet, feet with architectural deformities, and feet with ligament injuries.[23–25,27] This methodology on MR images with a voxel size of about $0.7 \times 0.7 \times 2.0$ mm was shown to have an accuracy and precision on the order of 1 voxel in both translation (1–2 mm) and rotation (1°–2°).

For traction, the primary motion of interest was axial translation. Axial translation was determined by measuring the change in distance along the z-axis between vertebral centroids. Coupled anterior-posterior translation and flexion-extension bending were also quantified for applied traction. For flexion-extension, sagittal plane rotation was the primary motion, with associated coupled axial displacement and anterior-posterior translations determined. Bending angles were calculated as the change in angle between the principal axes of respective vertebrae. The Euler angle order of decomposition was first about the y-axis, then about the z-axis, and lastly about the x-axis. Motions represent those of the superior relative to the inferior vertebrae. Means and standard deviations of all motions were calculated at each load increment.

All vertebral segmentations were performed by a single operator (S.L.S.). Selected series were resegmented to quantify errors associated with subjectivity in the segmentation process. Accordingly, any estimated spinal motion between the original and resegmented series represented the segmentation error. Accuracy of the entire positioning, imaging, and estimation using 3DVIEWNIX was determined by using radio-opaque markers of known dimensions attached to bones that underwent translations and rotations imposed by the test frame. For this, two bones of a single isolated ligamentous joint were used. Skin and soft tissue were removed,

and only muscle tissue directly attached to bones were left intact. To enable imposition of distraction and rotation between the bones of the joint, all ligaments and soft tissue connecting the joint were transected. This permitted independent movement of the bones relative to each other. A single marker was placed in each bone with minimal disruption of the soft tissue surrounding the bone. CT scans of these markers were acquired during prescribed translations and rotations and analyzed in the same manner as used for bone segmentation and motion analysis. Results were compared with motions directly measured during testing, and errors were determined as the differences between values determined by 3DVIEWNIX and those measured.

To assess the regional differences in spinal motion, the spine was divided into four segments: upper cervical spine (C1–C3), middle cervical spine (C3–C5), lower cervical spine (C5–C7), and CTJ (C7–T2). "C-spine" was designated as C1–C7 to evaluate these techniques for quantifying cervical spine motions and to compare the motions of cervical and CTJ regions. C-spine motion was calculated as the sum of the upper, middle, and lower segmental kinematic data.

To determine the tensile stiffness of the spinal regions, a linear regression through zero was fit to the force-displacement data for each specimen. Tensile stiffness for each specimen was defined as the linear coefficient of these fits. Stiffnesses were averaged across specimens and reported for each spinal region. To compare spinal regions, stiffness was multiplied by the number of motion segments in a region. For example, the upper spine is composed of two motion segments: C1–C2 and C2–C3. For sagittal bending, rotation angles were compared at the extreme of applied head rotations in both flexion and extension. All comparisons were made between spinal regions by using ANOVA, with significance defined at $P < 0.05$.

## ■ Results

Application of sCT techniques for tracking spine motions produced small errors (0.11 ± 0.12 mm) in translation measurements when considering specimen positioning, CT imaging, vertebral surface analysis, and motion calculations. Errors associated with only the image analysis techniques (mainly segmentation) were 0.11 ± 0.09 mm, contributing the greatest portion of the overall error in measurement. Likewise, mean errors in quantifying vertebral rotations were 0.9° ± 0.3° and 0.8° ± 0.7° for primary and coupled rotations, respectively. These analysis errors were small compared with motions in the primary direction of loading for this study.

Cervical traction applied to the head produced variable amounts of distraction for these spinal regions (Figure 3A). The CTJ exhibited the least amount of translation (0.32 ± 0.68 mm) in the superior-inferior direction along the long axis of the spine. In contrast, the C-spine underwent 3.08 ± 2.37 mm of translation at 178 N of load (Figure 3A). Average traction responses for all regions of the cervical spine exhibited a stiffening response typical of biologic tissue under load (Figure 3). However, the CTJ displayed very little translation, with a toe region up to 133 N, followed by only a very slight displacement. In traction, coupled sagittal plane rotations were small (<1°) for all regions, with the exception of the middle region where rotations increased nonlinearly to a maximum of 5.9° ± 5.0° (Figure 3B). While all cervical regions displayed coupled flexion, the CTJ underwent extension (0.63° ± 1.67° at 178 N) for traction applied to the head (Figure 3B).

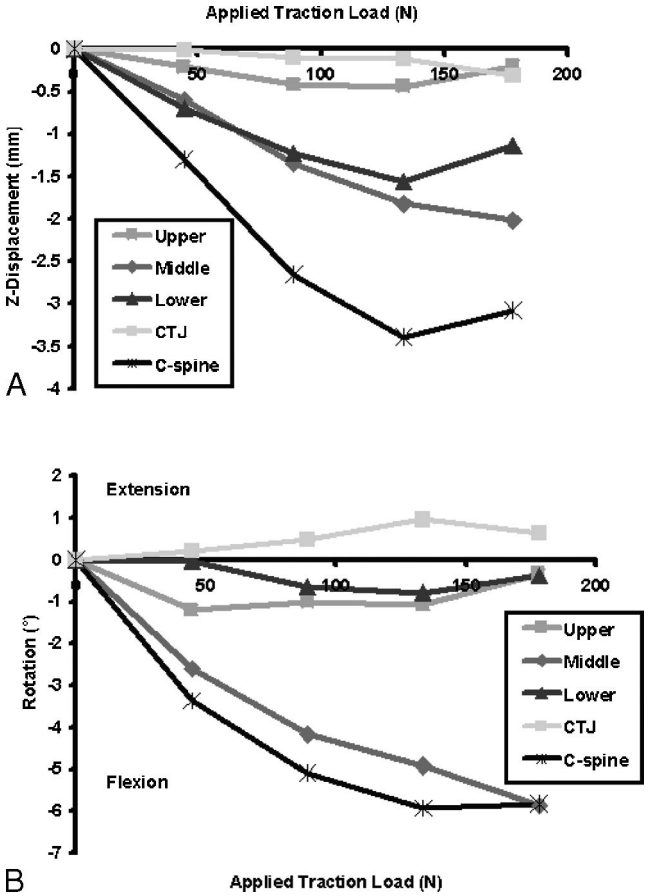


Figure 3. Average spinal motions in the sagittal plane produced for applied head traction shown by spinal region (upper, middle, lower, CTJ). Also shown is the response for the entire cervical spine (C-spine) for comparison to the CTJ responses. **A**, The CTJ exhibited the least axial displacement, indicating its high tensile stiffness in this load range. In contrast, C-spine displacement responses exhibited a typical stiffening response. **B**, Small coupled sagittal plane rotations were also produced for applied head traction, with the CTJ rotations remaining below 1° and the middle cervical spine demonstrating the greatest rotation in flexion. For rotation, negative angles indicate relative flexion; positive values indicate relative extension.

Estimated linear traction stiffness varied among spinal regions (Table 2), with the CTJ being the stiffest (779 N/mm) of any region and nearly 2.5 times that of the entire C-spine (317 N/mm) for these loads. For this traction range, the upper spine was the least stiff of all regions and the lower the most stiff. Despite variation in regional linear stiffnesses, differences were not significant ($P > 0.05$) between any regions.

For sagittal bending, CTJ rotations generally followed the lower cervical spine's behavior for small head rota-

**Table 2. Average Regional Spine Stiffnesses in Traction**

| Region | Stiffness (N/mm) | Motion Segments | Motion Segment Stiffness (N/mm) |
|---|---|---|---|
| Upper cervical spine (C1–C3) | 60 ± 314 | 2 | 119 ± 628 |
| Middle cervical spine (C3–C5) | 104 ± 48 | 2 | 208 ± 95 |
| Lower cervical spine (C5–C7) | 176 ± 169 | 2 | 351 ± 338 |
| Cervical spine (C1–C7) | 53 ± 19 | 6 | 317 ± 116 |
| CTJ (C7–T2) | 389 ± 826 | 2 | 779 ± 1652 |

Stiffness values were multiplied by the no. of motion segments to determine average stiffness for a motion segment in that region.

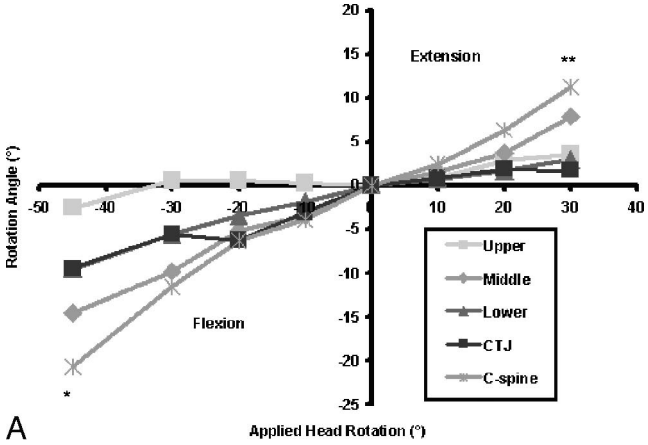


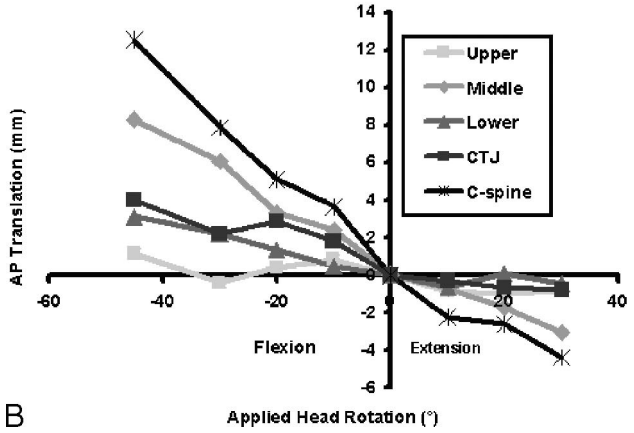


Figure 4. Average sagittal plane spinal motions produced for applied head rotation according to each spinal region (upper, middle, lower, CTJ, C-spine). **A**, Primary sagittal rotations (flexion, extension) of the CTJ followed those of the lower cervical spine and remained the lowest of all regions at the extreme head rotations. Primary CTJ rotations were significantly lower than the middle cervical spine at 45° of flexion (*$P = 0.045$) and at 30° of extension (**$P = 0.02$). **B**, Coupled anteroposterior displacement for applied head rotation was similar for the lower and CTJ spine regions and not different from each other, with the greatest motion occurring in the middle cervical spine for these head kinematics. Flexion angles are negative in magnitude; extension angles are positive.

tions (Figure 4A). For imposed head flexion, all cervical regions, including the CTJ, displayed increasing flexion rotation. The CTJ experienced less flexion than did the middle or entire C-spine regions. Indeed, these differences in flexion angle between the CTJ and other spinal regions were significant at 45° of flexion ($P = 0.045$) compared with the middle spine. For head extensions below 20°, the CTJ and lower spine rotations were similar; yet the CTJ began to display decreased flexibility at higher rotations, with a reduced range of motion compared with all other cervical regions at 30° (Figure 4A). At 30° extension, the CTJ had a significantly smaller range of motion compared with the middle region ($P = 0.02$). For all loading, anteroposterior translations followed rotations, according to normal coupling in the sagittal plane. For head flexion-extension, CTJ coupled translations were small, with mean values of 4.0 ± 1.3 mm for flexion and −0.8 ± 0.9 mm for extension (Figure 4B).

## ■ Discussion

To date, few studies have reported information on the kinematics of the CTJ. While existing work primarily provides insight into relative effectiveness of different fixation techniques for instrumenting the cervicothoracic junction,[10,17,18] the findings reported here are the first to our knowledge reporting any *in situ* data for the uninjured CTJ. Application of sCT techniques provides unique utility to quantify spinal kinematics and range of motion for the CTJ due to challenges in visualizing the C7 and T1 vertebrae with typical planar radiography approaches used in the cervical spine. Here we report mean axial translation of 0.32 mm for 178 N of applied traction at the head, which is approximately one half the value of the adjacent lower cervical spine (1.14 mm) and even less than the motion for the entire cervical spine (3.08 mm) for these loads (Figure 3A). Differences in regional mechanical behavior are also apparent in the tensile motion segment stiffnesses, with the CTJ (779 N/mm) being over twice as stiff as other cervical spinal regions (Table 2). In contrast, for applied head rotation, the CTJ demonstrates angular ranges of motion, which more closely follow those of the lower cervical spine (Figure 4A) and are less profound than those of the middle or entire cervical spine. Considering the small errors associated with the determined translational (~0.1 mm) and angular (<1°) motion components, the derived kinematic data can be considered reliable. Of note, continued efforts are needed to further develop and use test frames and loading paradigms for this application that have additional physiologic relevance. For example, it is recognized that the test frame used in this study may not impose clinically relevant vertebral bending. Also, the methods used here for error measurement do not fully simulate the *in situ* configuration used in our study or the *in vivo* clinical scenario. The effects of intact soft tissue would greatly reduce motions; yet the quantification of the ability of the segmentation technique to distinguish bone from soft tissue remains informative in interpreting the reported findings. Efforts are ongoing to both further

reduce these errors and improved their quantification for this and other imaging techniques.

This study is the first to report a CTJ tensile stiffness and associated ranges of motion and coupled sagittal motions for head flexion-extension. As such, it should be noted that the overall cervical spine motion segment stiffness determined here compares well with previous reports. Using isolated cadaveric cervical spine specimens, Van Ee *et al* reported a stiffness of 253 N/mm for ligamentous cervical spine motion segments.[20] Similarly, Shea *et al* found tensile cervical motion segment stiffness ranging from 157 to 433 N/mm.[28] Using sCT methods, the average stiffness for a single cervical spine motion segment was found to be 317 N/mm, which is within the range of values reported in the literature. Moreover, the average CTJ range of motion in flexion-extension determined here is approximately 12° (Figure 4A). Sagittal bending ranges of motion compare favorably with those compiled from human volunteer active and passive responses and *in vitro* cadaveric testing.[29] For example, while this method determined a range of motion for the lower cervical spine to be 12.5° (Figure 4A), our study incorporates passive musculature only and is limited to the head rotations of 75° inclusively. Not surprisingly, these angles are lower than those reported for that spinal region using active volunteers (37°).[29] Our findings further highlight the approach presented here as reliable and much-needed for *in situ*, and potentially even *in vivo*, applications for otherwise challenging imaging context.

The results of this study indicate that the cervicothoracic junction is a unique region of the cervical spine. It has much greater stiffness than its immediately superior counterpart (lower spine) and also displays coupled extension rotation for this mode of loading, while the lower cervical spine undergoes flexion (Figure 3B). Not surprisingly, the CTJ does not undergo a great deal of rotation in either flexion or extension (Figure 4B); its behavior for this loading follows almost directly that of the lower cervical spine. All other coupled motions (data not shown) for these studies are small for the CTJ and within the range of error detection, further implying that this region is quite stiff. Future investigations of CTJ mechanics outside the ranges of loading used here would provide additional insight into its mechanical behavior. Also, investigations of other physiologically relevant motions such as axial rotation and lateral bending would be beneficial in characterizing CTJ biomechanics. Moreover, it should be noted that the findings reported here, while *in situ* and including passive musculature for the intact cadaver, do not represent those conditions where active musculature is incorporated. However, data derived from the intact cadaver, as presented, provide an improved representation of the *in vivo* condition. As such, we provide a normative data set for this spinal region, which has remained otherwise absent in the literature.

These findings provide support for the implementation of sCT techniques to define *in vivo* biomechanical data in future applications. However, based on this work, modifications are required for improved utility in both the clinical and analysis aspects of these efforts. For example, using volunteer subjects would provide greater insight into the *in vivo* scenario. It would be desirable to implement these analysis techniques for use with MRI to remove patient radiation exposure. Also, current techniques require individual segmentation of each vertebra in each loading condition, introducing subjectivity (although the compromise in precision of this method due to this aspect is insignificant), as well as being highly time-intensive. This current limitation can be improved with automated segmentation techniques, further facilitating these methods for use in the clinical setting and is the focus of ongoing efforts.

While methods presented here demonstrate potential for defining biomechanical behavior of the spine and have previously been used with the ankle and foot,[23–25] they also offer a unique mathematical approach for detecting altered motions in spinal joints. Indeed, use of similar methods in the ankle has shown that examination of the association between architectural and geometric parameters of the bones in a joint can be used as a sensitive diagnostic tool for instability.[27] Such a quantitative approach for detecting potential soft tissue injuries in the spine would provide a novel method for diagnosing otherwise nondetectable injuries. Moreover, these techniques could also provide objective methods of evaluating the presence of a solid fusion or a pseudarthrosis in the postcervical fusion patient. Both of these applications remain currently unexplored in the spine because of limitations in imaging techniques and quantification of motion, among other factors. As modifications continue with the technologic and mathematical aspects of these techniques, it may be possible to use simpler techniques, such as stress radiography in selected planes (or even sCT in only selected planes), if it is determined that translation in or rotation about a particular plane carries the most sensitive clinical information.

sCT techniques provide a useful tool for biomechanical evaluation of the spine and, in particular, the CTJ. It has remained difficult to define biomechanical behavior of the cervicothoracic junction; this technique has proven useful for characterizing both its tensile stiffness and ranges of motion for clinically relevant loading scenarios. Further, the CTJ is much stiffer than other cervical regions (Figures 3, 4; Table 2), truly acting as a transition to the much stiffer thoracic spine. In addition, this study has determined that the coupled sagittal rotations in the CTJ for traction are directed oppositely to those of any other regions in the cervical spine, further suggesting a uniqueness for these joints. Such *in situ* findings would not be otherwise measurable using traditional techniques and suggest even more utility for sCT in defining motions and mechanical responses for the CTJ and entire spine for nonsagittal loading, both normal and in the case of injury.

***Acknowledgments***

The authors thank Tad Iwanaga for his help with installing the 3DVIEWNIX software on a laptop computer.

**■ Key Points**

- Kinematic CT methods are useful for studying cervicothoracic junction motions for clinically relevant applications.
- The cervicothoracic junction is nearly twice as stiff as other cervical spine regions and behaves as a distinct region in tension.
- For sagittal bending, the cervicothoracic junction follows the response of the lower cervical spine, acting as an extension of that region for that type of loading.

## References

1. Antonaci F, Ghirmai S, Bono G, et al. Current methods for cervical spine movement evaluation: a review. *Clin Exp Rheumatol* 2000;18(suppl):45–52.
2. Bogduk N, Mercer S. Review paper: biomechanics of the cervical spine: I. Normal kinematics. *Clin Biomech* 2000;15:633–48.
3. Bogduk N, Yoganandan N. Biomechanics of the cervical spine: Part 3. Minor injuries. *Clin Biomech* 2001;16:267–75.
4. Cassidy JD, Carroll LJ, Cote P, et al. Effect of eliminating compensation for pain and suffering on the outcome of insurance claims for whiplash injury. *N Engl J Med* 2000;342:1179–86.
5. Goldberg W, Mueller C, Panacek E, et al. Distribution and patterns of blunt traumatic cervical spine injury. *Ann Emerg Med* 2001;38:17–21.
6. Grauer JN, Panjabi MM, Cholewicki J, et al. Whiplash produces an S-shaped curvature of the neck with hyperextension at lower levels. *Spine* 1997;22:2489–94.
7. Kaneoka K, Ono K, Inami S, et al. Motion analysis of cervical vertebrae during whiplash loading. *Spine* 1999;24:763–9; discussion 70.
8. Panjabi MM, Nibu K, Cholewicki J. Whiplash injuries and the potential for mechanical instability. *Eur Spine J* 1998;7:484–92.
9. Breen A, Allen R, Morris A. A digital videofluoroscopic technique for spine kinematics. *J Med Eng Technol* 1989;13:109–13.
10. Bueff HU, Lotz JC, Colliou OK, et al. Instrumentation of the cervicothoracic junction after destabilization. *Spine* 1995;20:1789–92.
11. Ireland AJ, Britton I, Forrester AW. Do supine oblique views provide better imaging of the cervicothoracic junction than swimmer's views? *J Accid Emerg Med* 1998;15:151–4.
12. Jelly LM, Evans DR, Easty MJ, et al. Radiography versus spiral CT in the evaluation of cervicothoracic junction injuries in polytrauma patients who have undergone intubation. *Radiographics* 2000;20(suppl):251–9.
13. Dimnet J, Pasquet A, Krag MH, et al. Cervical spine motion in the sagittal plane: kinematic and geometric parameters. *J Biomech* 1982;15:959–69.
14. Karhu JO, Parkkola RK, Komu ME, et al. Kinematic magnetic resonance imaging of the upper cervical spine using a novel positioning device. *Spine* 1999;24:2046–56.
15. Panjabi MM, Duranceau J, Goel V, et al. Cervical human vertebrae: quantitative three-dimensional anatomy of the middle and lower regions. *Spine* 1991;16:861–9.
16. Winkelstein BA, Myers BS. Importance of nonlinear and multivariable flexibility coefficients in the prediction of human cervical spine motion. *J Biomech Eng* 2002;124:504–11.
17. Kreshak JL, Kim DH, Lindsey DP, et al. Posterior stabilization at the cervicothoracic junction: a biomechanical study. *Spine* 2002;27:2763–70.
18. Vaccaro R, Conant RF, Hilibrand AS, et al. A plate-rod device for treatment of cervicothoracic disorders: comparison of mechanical testing with established cervical spine in vitro load testing data. *J Spinal Disord* 2000;13:350–5.
19. Panjabi MM, Crisco J, Vasavada A, et al. Mechanical properties of the human cervical spine as shown by three-dimensional load-displacement curves. *Spine* 2001;26:2692–700.
20. Van Ee C, Nightingale R, Camacho D, et al. Tensile properties of the human muscular and ligamentous cervical spine. *44th Stapp Car Crash Conference Proceedings* 2000;85–102.
21. Ishii T, Mukai Y, Hosono N, et al. Kinematics of the upper cervical spine in rotation. *Spine* 2004;29:E139–44.
22. Ishii T, Mukai Y, Hosono N, et al. Kinematics of the subaxial cervical spine in rotation in vivo three-dimensional analysis. *Spine* 2004;29:2826–31.
23. Udupa JK, Hirsch BE, Samarasekera H, et al. Analysis of *in vivo* 3-D internal kinematics of the joints of the foot. *IEEE Trans Biomed Eng* 1998;45:1387–96.
24. Stindel E, Udupa J, Hirsch B, et al. An in vivo analysis of the motion of the peri-talar joint complex based on MR imaging. *IEEE Trans Biomed Eng* 2001;48:236–47.
25. Siegler S, Udupa JK, Ringleb, SI, et al. Mechanics of the ankle and subtalar joints revealed through a three-dimensional stress MRI technique. *J Biomech* 2005;38:567–78.
26. Udupa JK, Odhner D, Samarasekera S, et al. 3DVIEWNIX: an open, transportable, multidimensional, multimodality, multiparametric imaging software system. *Proc Soc Photo-Opt Eng* 1994;2164:58–73.
27. Stindel E, Udupa J, Hirsch B, et al. A characterization of the geometric architecture of the peritalar joint complex via MRI: an aid to classification of foot type. *IEEE Trans Biomed Eng* 1999;18:753–63.
28. Shea M, Edwards WT, White AA, et al. Variations of stiffness and strength along the human cervical spine. *J Biomech* 1991;24:95–107.
29. White AA, Panjabi MM. *Clinical Biomechanics of the Spine*. Philadelphia: Lippincott Williams & Wilkins, 1990.